ONECENTRAL PRESS

Available online at www.onecentralpress.com

One Central Press

journal homepage: www.onecentralpress.com/functional-nanostructures

Molecular Dynamics Study of Protein Deformation through Solid-State Nanopore

Mohammad Raziul Hasan,[a,b,c] Mohammed Arif I. Mahmood,[a,b,c] Raja Raheel Khanzada,[a,b,c] Nuzhat Mansur,[a,b,c] Ashfaq Adnan,[d] and Samir M. Iqbal[e,f,]*

[a]Nano-Bio Lab; [b]Nanotechnology Research Center; [c]Department of Electrical Engineering; [d]Department of Mechanical and Aerospace Engineering, University of Texas at Arlington, Arlington, Texas 76019, USA; [e]Department of Electrical Engineering, [f]School of Medicine, University of Texas Rio Grande Valley, Edinburg, Texas 78539, USA.
[*]Corresponding author

ABSTRACT

Electrophoretic translocation through solid-state nanopores is a promising technique for identification of specific proteins and protein complexes. In a typical protein detection experiment, an external electric field (e-field) is applied across the nanopore and the ionic current is measured while the molecule passes through the pore. It is very important that the protein retains its structure and functionality under applied e-field and experimental conditions. However, the elongation and deformation of the 3D structure may bias the detection scheme. This work presents a theoretical assessment of protein deformation in a nanopore experiment due to applied e-field. We used nanoscale molecular dynamics (NAMD) simulations to investigate the deformation of a model protein during translocation through a silicon nitride nanopore in an aqueous solution under varying e-fields. We simulated the experimental conditions and performed quantitative analysis of the variations in thrombin protein's 3D structure. No mechanical force was applied on the protein to ensure the sole contribution of e-field on the deformation. The conformational changes of thrombin's structure were quantified in terms of root mean square deviation (RMSD) and radial distribution function. It was observed that large voltages resulted in deformations in protein structure. The protein molecule got stretched under the influence of high e-field as it traveled through nanopore. The interaction mechanism between nanopore and protein is crucial to understand the detection dynamics. The results can guide better design of experiments with proteins confined in a nanopore.

I. INTRODUCTION

Over the past decade, nanopore technology has advanced substantially due to its capability for single molecule detection and characterization [1-5]. Nanopore devices have been used for label free detection of DNA [6], RNA [7, 8], and also for rapid nucleic acid sequence detection [9-11]. It is also an attractive choice for sensitive and accurate detection of proteins and protein-complexes [1, 12, 13]. Here, we explore the structural deformations of a protein translocating through a nanopore.

Most of the early nanopore studies were done with biological nanopores like alpha-hemolysin or Mycobacterium smegmatis porin A (MspA) [9, 14]. Solid-state nanopores emerged as an alternative choice and became more popular for their robustness, easy fabrication, high throughput, low cost, and scalability [5]. In the past decade, synthetic nanopores have been widely used for single molecule detection [2, 15-17]. Although silicon nitride (Si_3N_4) is the most popular choice of material for synthetic nanopores [13, 15, 18, 19], other materials such as silicon dioxide (SiO_2) [16, 20], aluminum-oxide (Al_2O_3) [17], and graphene [21-24] have also been used to make nanopores. Several studies have been conducted on protein translocation through solid-state nanopores including protein transport [25], protein identification [13, 26], unfolding and stretching of proteins [27], protein trapping [14], high voltage transport of protein [25], and localization of proteins in a DNA [28]. In some cases, the inner wall of the nanopore is engineered with other biomaterials to mimic the biological ion channels [29]. Lipid coated nanopore has been used to tailor protein translocation [30], aptamer coating on nanopore wall has been used for increased selectivity [31], chemical modification and metallization have been done for stochastic sensing of proteins [26].

The structural integrity of proteins is a common concern during the nanopore-based detection process [15]. The stress caused by channel constriction during translocation or applied e-field may deform the 3D shape of protein. Recent studies have shown that the biophysical properties of a protein are manipulated by variations in solvent conditions or pH in a nano-confined environment [15, 32]. In addition, thermal/chemical changes, and

e-field can influence interactions between the protein and pore which can trigger protein denaturation inside a nanopore [33]. Thus, a comprehensive understanding of the conformational changes is important because of the nature of detection using ionic current measurement. Study of the deformation can be a stepping stone for a comprehensive understanding of the orientation and interactions of the constituting amino acids of the protein. Computational analysis and simulation tools provide advantages in such cases because these explore atomic level interactions which are rather difficult to grasp from experimental situations [34]. Several theoretical and computational analyses such as coarse grained dynamic simulations [35], time distribution models [19], molecular dynamics [36, 37], and stochastic models [38] have been designed to study the translocation behavior and dynamics of protein molecule inside a nanopore [39]. Similar studies on deformation mechanism for DNA have been presented already [40-43]. In our prior work, we have shown the deformability of DNA structure under electric bias [44].

In this paper, we present the deformation of a protein inside a nanopore under the influence of applied bias. This is valuable for protein detection experiments with nanopores as the function of a protein depends on the integrity of its conformal structure [45]. We have used Nanoscale Molecular Dynamics (NAMD v2.9) to simulate the translocation of protein through a Si_3N_4 pore and observed the deformations of protein structure [46]. Thrombin was used as a model protein. The 3D structural deformation of the protein was measured using Visual Molecular Dynamics (VMD v1.9.2) while varying e-fields were applied across the pore [47]. Thrombin is the protein responsible for thrombosis. Thrombin plays a vital role in cancer metastasis as well [48]. No mechanical force was used on the protein to ensure that only the influence of applied bias on the deformation was monitored. We simulated the system for 20 ns of translocation of protein using a multicore computing facility at Texas Advanced Computing Center (TACC) and analyzed the structural changes for applied voltages. Root mean square deviation (RMSD) and radial distribution function (RDF) were measured from VMD and used to quantify the deviation of protein structure from its initial structure. The protein deformed gradually with the increase in e-field and although the overall size of the protein did not significantly change at smaller voltages, the shape got stretched due to the presence of e-field. The MD simulations provided insights that can be used to optimize experiments that investigate protein translocation through nanopores.

The basic principal of molecular translocation through a nanopore is very straight forward. A schematic is shown in Fig. 1. The experimental setup includes two chambers separated by a solid state nanopore. Typically the nanopore is drilled by high energy electron beam of transmission electron microscope (TEM) or by using focused ion beam (FIB) [16]. Although the ion beam has higher energy compared to electron-beam to drill a pore in a thicker membrane, a TEM offers better control and precision over the pore diameter because the size of the electron beam is much smaller than that of the ion beam used in FIB.

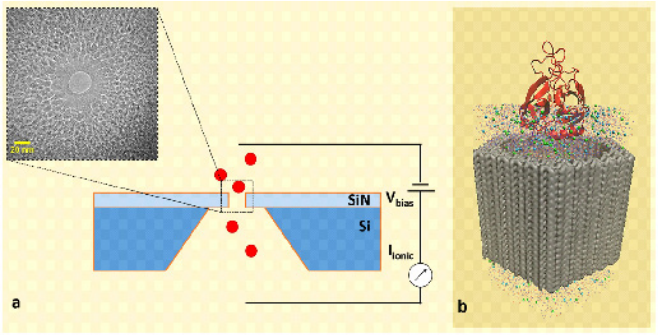

Figure 1 (a) Schematic representation of nanopore experiment to capture the ionic current signature for protein translocation, inset shows an actual TEM drilled nanopore. (b) Model of the simulated system: all-atom MD model comprised of a thrombin inside a Si_3N_4 nanopore. The pore is solvated with KCl. The inner diameter of the pore is 6 nm, simulated periodic cell structure is 68 Å× 78 Å × 96 Å.

In a nanopore measurement setup, chip with nanopore is sandwiched between two chambers. The chambers are filled with buffer solution and electrodes are placed in the chambers to create an e-field high enough to force the target molecules to pass from one chamber to the other through the nano-aperture. The ionic current is measured with patch-clamp measurement system. When a molecule travels through the nanopore, a drop in the ionic current is registered. This current profile gives insights on the properties of the molecule. The magnitude and duration of the current blockade are proportional to the size and the transition time of the passing analyte through the pore. In some cases, the pore is smaller than the molecule to measure the mechanophysical properties of the translocating molecule. Fig. 1 shows a cross section of a Si_3N_4 nanopore and a protein crossing the pore due to applied bias.

II. MATERIALS AND METHODS

Simulation Details. We used NAMD v2.9 to simulate the experiment [46]. VMD v1.9.2 was used for visualization and data analysis of the simulated results [47]. The protocol for MD model is similar to the one reported by Aksimentiev et al. [49]. CHARMM22 model was used for the force field calculations [50, 51]. All simulations were performed on computer clusters that had 6400 nodes each configured with two Xeon E5-2680 processors and one Intel Xeon Phi SE10P Coprocessor (on a PCIe card). Each node was configured with 32GB of 'host' memory with an additional 8GB of memory on the Xeon Phi coprocessor card, at Texas Advanced Computing Center (TACC) using 240 cores in parallel.

The structure of thrombin was obtained from the Research Collaboratory for Structural Bioinformatics (RCSB). The protein data bank (PDB) file, 1HAP, contained the x-ray resolved configuration of a thrombin-oligomer complex [52]. VMD was used to extract the structure of human alpha thrombin. The protein had two major chains, chain-L and chain-H with 36 and 259 amino acids, respectively. The nanopore diameter was selected to be slightly larger than the protein size to negate the effects of protein deformation due to nanopore constriction. The pore was placed in the z-direction and the protein was electrophoretically driven through the nanopore.

Model Construction. The simulation consisted of a 6 nm thick block of Si_3N_4 containing a 6 nm diameter nanopore at the center. First, a crystalline structure of Si_3N_4 unit cell was created. Then the unit cell was replicated and assembled in order to form a 10 nm x 10 nm x 6 nm Si_3N_4 membrane. Since the longest dimension of thrombin is 4.7 nm in its native state, a 6 nm diameter nanopore was created at the center of the membrane. The membrane was given a hexagonal shape to reduce the total number of atoms, ensuring better simulation speed. The atom count for the complete nanopore model was 11,016. The pore was solvated with 1M KCl solution. Salt concentration was chosen close to standard experimental conditions [53]. Since no mechanical force was applied, the protein was electrophoretically driven through the nanopore.

Each simulation was executed in three steps. First, the total system energy was minimized by conjugate gradient method to ensure a stable system. Energy minimization involved finding the minimum energy landscape where the molecule was relaxed. This was achieved by systematically varying the positions of atoms and calculating the energy in an iterative manner. Then the temperature of the system was raised to 295 K gradually at constant volume (i.e. in NVT ensemble) followed by an equilibration at constant pressure and temperature (i.e. NPT ensemble). Finally, an electric potential was applied across the nanopore along the z-axis at constant volume. The simulation was performed for 20 ns at 1 fs steps. The applied e-field was varied from 0 to 1 kCal/(mol.Å.e) for each system using equation (1) [49]. The trajectory frames were recorded every 800 fs in 20 ns duration.

$$E-field_z\left(kCal/mol.\mathring{A}.e\right)=\frac{-23.060549x\ U}{l_z}\left(V/\mathring{A}\right) \quad (1)$$

Here, U is the potential difference and l_z is the size of the whole system along the z-axis. The NAMD unit for e-field is kCal/(mol.Å.e), where 23.0605492 is the conversion factor for U (volts) and l_z (angstroms).

Force-field Calculations. The interatomic and intermolecular force fields were estimated with CHARMM22 and CHARMM27 models because these are noteworthy for protein and DNA systems, respectively. The CHARMM22 model used a potential energy function *U(R)*, as defined by equation (2) [50].

$$\begin{aligned}U(R)=&\sum_{bonds}K_b\left(b-b_0\right)^2+\sum_{UB}K_{UB}\left(S-S_0\right)^2+\sum_{angle}K_\theta\left(\theta-\theta_0\right)^2\\&+\sum_{dihedrals}K_\chi\left(1+\cos\left(n\chi-\delta\right)\right)+\sum_{impropers}K_{imp}\left(\varphi-\varphi_0\right)^2\\&+\sum_{nonbond}\in_{ij}\left[\left(\frac{R_{\min_{ij}}}{r_{ij}}\right)^{12}-\left(\frac{R_{\min_{ij}}}{r_{ij}}\right)^{6}\right]+\frac{q_iq_j}{\in_1 r_{ij}}\end{aligned} \quad (2)$$

Where, K_b, K_{UB}, K_θ, K_χ, K_{imp} are the force constants associated with bonds, Urey-Bradley, angles, dihedrals, and improper dihedral angles, respectively. The variables b, S, θ, χ, φ, n, and δ represent the bond length, Urey-Bradley-distance, bond angle, dihedral angle, improper torsion angle, phase shift, and multiplicity or periodicity of the dihedral angle, respectively. The last two terms of the equation describe the van der Waals energy calculated with Lennard-Jones potential and the electrostatic energy assessed from Coulombic potential. Here $\in$ and r_{ij} are effective dielectric constant, and distance between atoms i and j, respectively. The $\in_{ij}$ values were established by the geometric mean of $\in_i$ and $\in_j$, and $R_{\min_{ij}}$ values were calculated from the arithmetic mean of $R_{\min_i}$ and $R_{\min_j}$.

III. RESULTS AND DISCUSSION

The thrombin molecule was placed inside the nanopore and the change in its structure was observed for increasing electric potentials applied across the nanopore. The e-field was set to 0.0, 0.05, 0.10 and 1.0 kCal/(mol.Å.e) along the z-axis. The deformation was quantified by the RMSD of protein backbone from its initial conformation having the two structures in best alignment with each other. The formula for RMSD calculation is:

$$\begin{aligned}RMSD_\alpha\left(t_j\right)&=\sqrt{\frac{\sum_{\alpha=1}^{N_\alpha}\left(r_\alpha\left(t_j\right)-\langle r_\alpha\rangle\right)^2}{N_\alpha}}\\\langle r_\alpha\rangle&=\frac{1}{N_t}\sum_{j=1}^{N_t}r_\alpha\left(t_j\right)\end{aligned} \quad (3)$$

where N_α is the number of atoms whose positions are being compared. N_t is the number of time steps over which the positions are compared, $r_\alpha\left(t_j\right)$ is the position of atom α at time t_j and $\langle r_\alpha\rangle$ is the average value of the position of atom α. VMD was used to calculate the RMSD of the protein structure for each frame at every 0.8 ps interval for the total time span of 20 ns.

Fig. 2 shows the RMSD of thrombin's shape at increasing e-field. The deformation in thrombin's structure was insignificant for low e-fields such as 0.05 and 0.1 kCal/(mol.Å.e). At these voltages, the force fields were not strong enough to deform the protein's structure. Proteins are made of amino acids. The net charge of a protein depends on its isoelectric point (pI) and pH. In the presence of an e-field, the amino acids tend to reorder due to electrostatic forces to attain the lowest possible energy state. This resulted

in a slightly deformed structure of the molecule. Higher voltage would result in larger electrostatic force and cause more deformation. The results showed that an e-field as high as 1 kCal/(mol.Å.e) deformed the protein by approximately 16% from its initial structure within the first 20 ns. The trend of the deformation suggested that more deformation would occur for a longer exposure to this e-field. However, a high voltage in a nanopore experiment would reduce the protein translocation time to facilitate a high-throughput analysis but at the cost of further deformation in protein structure.

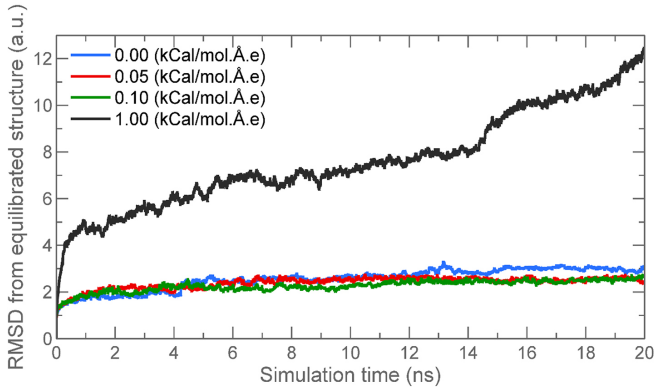

Figure 2 RMSD of the protein backbone compared with the initial conformation.

In typical nanopore experiments, protein molecules move through the nanopores due to their charge which in turn is defined by their pI and the pH of the solution in the presence of an e-field [54]. The pI of human thrombin is 7.0–7.6 [55]. Since the pH of the solution was ~7.0, the thrombin was slightly positively charged. As a result, it travelled towards the negative potential. A complete protein translocation event is approximately a few hundred microseconds to milliseconds [12, 13]. The simulations performed here were done for 20 ns. Although it was very short compared to typical experiments, it was possible to precisely monitor the movement even within 20 ns because of the detailed information captured. The center of mass (COM) of the molecule was calculated and the movement of the COM was tracked over time. The projections of the overall movement along the three axes (x, y and z) were then calculated. The correlation between the protein's overall movement and the projection in a particular axis was calculated to find the direction of movement. The maximum correlation coefficient (0.963 ± 0.025) was observed for the z-axis component for all three bias situations. This validated that the overall movement was along the z-axis which was the same direction for the applied e-field. The same was observed from the trajectory of the molecule in VMD.

The radial distribution function, $g(r)$, of thrombin's structure was also calculated to observe the distribution of the atoms of the protein and the effects of the external e-field on the distribution. In statistical mechanics, radial distribution function of a system describes the variations in the density of particles as a function of distance from a reference point. It is a useful tool that is utilized in molecular dynamics to describe the structure of a system. It measures the probability of finding a neighbouring atom with respect to distance from another one. The $g(r)$ of thrombin's 3D structure was computed by calculating the interatomic distance of every particle pair and by binning them in a histogram. The histogram was then normalized by the volume of a spherical shell with thickness, *δr*. This was achieved by multiplying the density function with the volume of a spherical shell at distance r, as shown in equation 4.

$$g(r) = \frac{1}{N}\frac{dn(r)}{4\pi r^2 dr\ \rho} \tag{4}$$

Here, *N* represents the total number of atoms, *ρ* is the number density, and *dn(r)* is the number of atoms at a distance *r* and *r+dr*.

The radial distribution analysis of the thrombin's structure at varying e-fields is shown in Figs. 3(a) and 3(b). The horizontal axis is the distance around an atom, while the vertical axis in Fig. 3(a) represents the number of atom-pairs present at a distance given on the x-axis. The position of the peak represents the most common distance between two atoms. At higher e-field, there is a right shift of the curve. That means the most probable distance between any two atoms increased approximately from 2.2 nm to ~2.6 nm due to the large e-field. Hence the atoms in the protein went apart from each other. The expansion of the curve along horizontal axis suggests that the protein got stretched under a higher e-field.

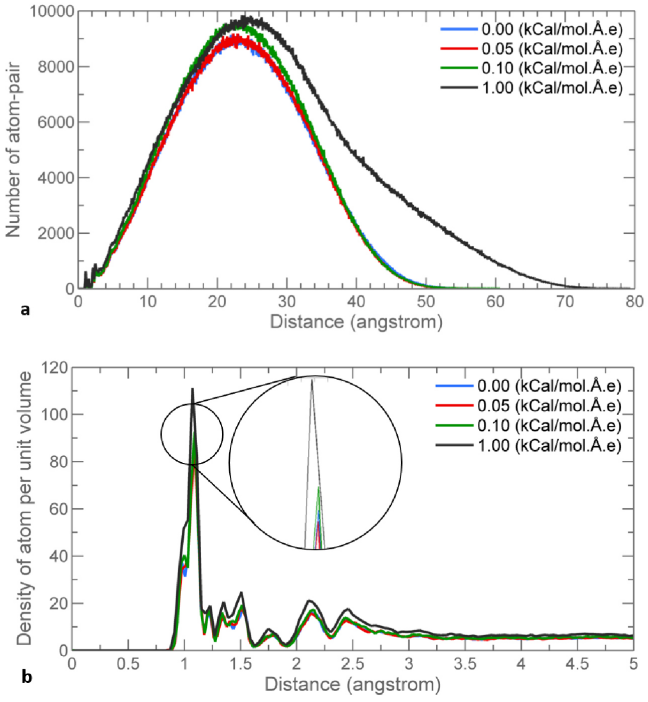

Figure 3 (a) Radial distribution analysis of thrombin's structure after 20 ns simulation at increasing e-field. The vertical axis represents the number of atom-pair at a distance mentioned in horizontal axis. (b) Normalized radial distributions function: the density of atoms lying on the surface of a sphere at the listed distance from an atom.

Fig. 3(b) is the normalized version of 3(a). The vertical axis here shows the number of neighboring atoms present in an imaginary sphere of that distance. The position of the prominent peak over here is around 1 Å, which refers to the radius of the imaginary sphere around an atom to have the highest atom density. There is no significant shift in the position of this peak. However the height of the dominant peak increased by approximately 20% from its initial position at the high e-fields. It means that at the very vicinity of an atom the neighboring atoms were more tightly packed in the presence of the higher e-field. This was again a result of stretched deformation.

To measure the effect of protein deformation on the ionic current profile, the average ionic current was measured through the pore. Ideally proteins are suspended in an ionic solution in the nanopore experiments. When there is no protein inside the nanopore, the setup only measures the ionic current from the movements of K^+ and Cl^- ions. This is registered as the baseline current. During translocation, the protein molecule block a certain amount of KCl ions through the cylindrical pore. This current blockage depends on the size and charge of the translocating molecule and also the charge of the K^+ and Cl^- atoms. The ionic current profiles for four e-fields (ranging from 0 to 1 kCal/(mol.Å.e)) were recorded. Since the state of the MD system was recorded after every 800 fs, the current profile was recorded from the change in total electric charge between two consecutive time-frames. These calculations were done for the entire 20 ns time span. Equation 5 represents the current calculation, where, z_i and q_i are z-coordinate and charge of ion i, respectively, and Δt is the simulation step [56]. The size of the whole system is defined by l_z along the z-axis as defined in Equation (1).

$$I\left(t+\Delta t/2\right)=\frac{1}{\Delta t\, l_z}\sum_{i=1}^{N} q_i\left(z_i\left(t+\Delta t\right)-z_i\left(t\right)\right); \qquad (5)$$

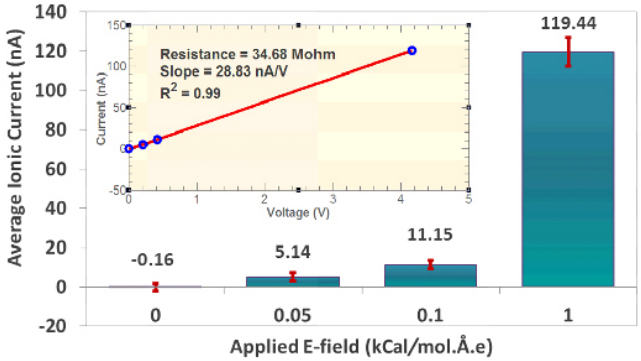

Figure 4 Current-Voltage profile of the system. The average ionic current shows linear dependence on the applied potential when the protein is inside the nanopore. Inset shows the linear relationship between the two entities. The data points are interpolated with linear regression analysis.

The current-voltage (*I-V*) profile of the system was calculated to understand the equivalent resistance introduced by the protein (Fig. 4). At higher e-field, more ions passed through the nanopore resulting in an increase in the current. It is visible from the plot that the nanopore current increased linearly as the applied voltage increased. The linear *I-V* profile suggests that the protein, while inside the nanopore, offered a constant resistance even when it was slightly deformed due to the e-field.

Fig. 2 (RMSD) and Fig. 3(a) (atom-pairs distribution) plots suggest that the protein showed deformation in the shape with more atomic packing. This led to an overall enlargement of the protein at a higher e-field. The protein went through stretching associated with the forces in the nanopore in response to high voltage. Since the force was exerted in the direction of travel, the structure got stretched in the same direction. This did not significantly affect the overall blocking of the pore and hence was not visible through the ionic current profile. This phenomenon may not be very crucial for nanopore experiments with DNA or polymer chains but should be considered for studying size sensitive biomolecules such as proteins.

IV. CONCLUSIONS

We have investigated a computational model for sensing protein translocations through nanopores. Using this model, we have studied the interatomic interactions and translocation of thrombin through a Si_3N_4 nanopore. The conformal structure of the protein that yields its particular functional form and also the alterations in protein structure are important to understand. A comprehensive analysis has been presented to quantify the behavior of a model protein inside a solid-state nanopore under external e-field. The protein underwent gradual deformation at high applied voltage. The structural deformability, atomic displacement, and ionic current for thrombin passing through a nanopore were quantified. The presented framework allows a closer inspection on the underlying processes of a nanopore experiment. This knowledge can be translated into design rules for protein measurement experiments with solid-state nanopores.

V. CONFLICT OF INTEREST DISCLOSURES

The authors made no disclosures.

VI. ACKNOWLEDGEMENTS

The authors gratefully acknowledge the Texas Advanced Computing Center (TACC) for supercomputing applications. This work was supported by National Science Foundation grant ECCS-1201878.

VII. REFERENCES

[1] S. Howorka and Z. S. Siwy, “Nanopores as

protein sensors," *Nature Biotechnology,* vol. 30, pp. 506-507, 2012.

[2] B. N. Miles, A. P. Ivanov, K. A. Wilson, F. Doğan, D. Japrung, and J. B. Edel, "Single molecule sensing with solid-state nanopores: novel materials, methods, and applications," *Chemical Society Reviews,* vol. 42, pp. 15-28, 2013.

[3] L. Movileanu, "Interrogating single proteins through nanopores: challenges and opportunities," *Trends in Biotechnology,* vol. 27, pp. 333-341, 2009.

[4] D. H. Stoloff and M. Wanunu, "Recent trends in nanopores for biotechnology," *Current Opinion in Biotechnology,* vol. 24, pp. 699-704, 2013.

[5] B. M. Venkatesan and R. Bashir, "Nanopore sensors for nucleic acid analysis," *Nature Nanotechnology,* vol. 6, pp. 615-624, 2011.

[6] M. Wanunu, W. Morrison, Y. Rabin, A. Y. Grosberg, and A. Meller, "Electrostatic focusing of unlabelled DNA into nanoscale pores using a salt gradient," *Nature Nanotechnology,* vol. 5, pp. 160-165, 2010.

[7] T. Z. Butler, J. H. Gundlach, and M. Troll, "Ionic current blockades from DNA and RNA molecules in the α-hemolysin nanopore," *Biophysical Journal,* vol. 93, pp. 3229-3240, 2007.

[8] T. Z. Butler, J. H. Gundlach, and M. A. Troll, "Determination of RNA orientation during translocation through a biological nanopore," *Biophysical Journal,* vol. 90, pp. 190-199, 2006.

[9] E. A. Manrao, I. M. Derrington, A. H. Laszlo, K. W. Langford, M. K. Hopper, N. Gillgren*, et al.*, "Reading DNA at single-nucleotide resolution with a mutant MspA nanopore and phi29 DNA polymerase," *Nature Biotechnology,* vol. 30, pp. 349-353, 2012.

[10] G. Sigalov, J. Comer, G. Timp, and A. Aksimentiev, "Detection of DNA sequences using an alternating electric field in a nanopore capacitor," *Nano Letters,* vol. 8, pp. 56-63, 2008.

[11] D. B. Wells, M. Belkin, J. Comer, and A. Aksimentiev, "Assessing graphene nanopores for sequencing DNA," *Nano Letters,* vol. 12, pp. 4117-4123, 2012.

[12] W. Ali, M. U. Raza, M. A. I. Mahmood, P. B. Allen, A. R. Hall, Y. Wan*, et al.*, "Differentiation of Specific Cancer Biomarkers with Solid-state Nanopores," *Functional Nanostructures,* pp. 26-34, 2016.

[13] A. Han, G. Schürmann, G. Mondin, R. A. Bitterli, N. G. Hegelbach, N. F. de Rooij*, et al.*, "Sensing protein molecules using nanofabricated pores," *Applied Physics Letters,* vol. 88, p. 3901, 2006.

[14] M. M. Mohammad, S. Prakash, A. Matouschek, and L. Movileanu, "Controlling a single protein in a nanopore through electrostatic traps," *Journal of the American Chemical Society,* vol. 130, pp. 4081-4088, 2008.

[15] D. Fologea, B. Ledden, D. S. McNabb, and J. Li, "Electrical characterization of protein molecules by a solid-state nanopore," *Applied Physics Letters,* vol. 91, p. 053901, 2007.

[16] A. Storm, J. Chen, X. Ling, H. Zandbergen, and C. Dekker, "Fabrication of solid-state nanopores with single-nanometre precision," *Nature Materials,* vol. 2, pp. 537-540, 2003.

[17] B. M. Venkatesan, B. Dorvel, S. Yemenicioglu, N. Watkins, I. Petrov, and R. Bashir, "Highly sensitive, mechanically stable nanopore sensors for DNA analysis," *Advanced Materials,* vol. 21, pp. 2771-2776, 2009.

[18] D. J. Niedzwiecki, R. Iyer, P. N. Borer, and L. Movileanu, "Sampling a biomarker of the human immunodeficiency virus across a synthetic nanopore," *ACS Nano,* vol. 7, pp. 3341-3350, 2013.

[19] C. Plesa, S. W. Kowalczyk, R. Zinsmeester, A. Y. Grosberg, Y. Rabin, and C. Dekker, "Fast translocation of proteins through solid state nanopores," *Nano Letters,* vol. 13, pp. 658-663, 2013.

[20] M. J. Kim, M. Wanunu, D. C. Bell, and A. Meller, "Rapid fabrication of uniformly sized nanopores and nanopore arrays for parallel DNA analysis," *Advanced Materials,* vol. 18, pp. 3149-3153, 2006.

[21] S. Garaj, W. Hubbard, A. Reina, J. Kong, D. Branton, and J. Golovchenko, "Graphene as a subnanometre trans-electrode membrane," *Nature,* vol. 467, pp. 190-193, 2010.

[22] C. A. Merchant, K. Healy, M. Wanunu, V. Ray, N. Peterman, J. Bartel*, et al.*, "DNA translocation through graphene nanopores," *Nano Letters,* vol. 10, pp. 2915-2921, 2010.

[23] G. F. Schneider, S. W. Kowalczyk, V. E. Calado, G. Pandraud, H. W. Zandbergen, L. M. Vandersypen*, et al.*, "DNA translocation through graphene nanopores," *Nano Letters,* vol. 10, pp. 3163-3167, 2010.

[24] B. M. Venkatesan, D. Estrada, S. Banerjee, X. Jin, V. E. Dorgan, M.-H. Bae*, et al.*, "Stacked graphene-Al_2O_3 nanopore sensors for sensitive detection of DNA and DNA–protein complexes," *ACS Nano,* vol. 6, pp. 441-450, 2011.

[25] B. Cressiot, A. Oukhaled, G. Patriarche, M. Pastoriza-Gallego, J.-M. Betton, L. Auvray*, et al.*, "Protein transport through a narrow solid-state nanopore at high voltage: experiments and theory," *ACS Nano,* vol. 6, pp. 6236-6243, 2012.

[26] R. Wei, V. Gatterdam, R. Wieneke, R. Tampé, and U. Rant, "Stochastic sensing of proteins with receptor-modified solid-state nanopores," *Nature Nanotechnology,* vol. 7, pp. 257-263, 2012.

[27] K. J. Freedman, S. R. Haq, J. B. Edel, P. Jemth, and M. J. Kim, "Single molecule unfolding and stretching of protein domains inside a solid-state nanopore by electric field," *Scientific Reports,* vol. 3, 2013.

[28] S. W. Kowalczyk, A. R. Hall, and C. Dekker, "Detection of local protein structures along

DNA using solid-state nanopores," *Nano Letters,* vol. 10, pp. 324-328, 2009.

[29] S. W. Kowalczyk, L. Kapinos, T. R. Blosser, T. Magalhães, P. van Nies, R. Y. Lim*, et al.*, "Single-molecule transport across an individual biomimetic nuclear pore complex," *Nature Nanotechnology,* vol. 6, pp. 433-438, 2011.

[30] E. C. Yusko, J. M. Johnson, S. Majd, P. Prangkio, R. C. Rollings, J. Li*, et al.*, "Controlling protein translocation through nanopores with bio-inspired fluid walls," *Nature Nanotechnology,* vol. 6, pp. 253-260, 2011.

[31] D. Rotem, L. Jayasinghe, M. Salichou, and H. Bayley, "Protein detection by nanopores equipped with aptamers," *Journal of the American Chemical Society,* vol. 134, pp. 2781-2787, 2012.

[32] D. Lucent, V. Vishal, and V. S. Pande, "Protein folding under confinement: a role for solvent," *Proceedings of the National Academy of Sciences,* vol. 104, pp. 10430-10434, 2007.

[33] K. J. Freedman, M. Jürgens, A. Prabhu, C. W. Ahn, P. Jemth, J. B. Edel*, et al.*, "Chemical, thermal, and electric field induced unfolding of single protein molecules studied using nanopores," *Analytical Chemistry,* vol. 83, pp. 5137-5144, 2011.

[34] A. Aksimentiev, R. Brunner, J. Cohen, J. Comer, E. Cruz-Chu, D. Hardy*, et al.*, "Computer Modeling in Biotechnology," *Nanostructure Design: Methods and Protocols,* pp. 181-234, 2008.

[35] P.-H. Lee, V. Helms, and T. Geyer, "Coarse-grained Brownian dynamics simulations of protein translocation through nanopores," *The Journal of Chemical Physics,* vol. 137, p. 145105, 2012.

[36] J. Gumbart and K. Schulten, "Molecular dynamics studies of the archaeal translocon," *Biophysical Journal,* vol. 90, pp. 2356-2367, 2006.

[37] S. K. Kannam, S. C. Kim, P. R. Rogers, N. Gunn, J. Wagner, S. Harrer*, et al.*, "Sensing of protein molecules through nanopores: a molecular dynamics study," *Nanotechnology,* vol. 25, p. 155502, 2014.

[38] C. Y. Kong and M. Muthukumar, "Simulations of stochastic sensing of proteins," *Journal of the American Chemical Society,* vol. 127, pp. 18252-18261, 2005.

[39] L. Javidpour, M. R. R. Tabar, and M. Sahimi, "Molecular simulation of protein dynamics in nanopores. I. Stability and folding," *The Journal of Chemical Physics,* vol. 128, p. 115105, 2008.

[40] J. B. Heng, A. Aksimentiev, C. Ho, P. Marks, Y. V. Grinkova, S. Sligar*, et al.*, "Stretching DNA using the electric field in a synthetic nanopore," *Nano Letters,* vol. 5, pp. 1883-1888, 2005.

[41] J. B. Heng, C. Ho, T. Kim, R. Timp, A. Aksimentiev, Y. V. Grinkova*, et al.*, "Sizing DNA using a nanometer-diameter pore," *Biophysical Journal,* vol. 87, pp. 2905-2911, 2004.

[42] J. Li, M. Gershow, D. Stein, E. Brandin, and J. Golovchenko, "DNA molecules and configurations in a solid-state nanopore microscope," *Nature Materials,* vol. 2, pp. 611-615, 2003.

[43] B. Luan, D. Wang, R. Zhou, S. Harrer, H. Peng, and G. Stolovitzky, "Dynamics of DNA translocation in a solid-state nanopore immersed in aqueous glycerol," *Nanotechnology,* vol. 23, p. 455102, 2012.

[44] M. A. I. Mahmood, W. Ali, A. Adnan, and S. M. Iqbal, "3D Structural Integrity and Interactions of Single-Stranded Protein-Binding DNA in a Functionalized Nanopore," *The Journal of Physical Chemistry B,* vol. 118, pp. 5799-5806, 2014.

[45] M.-J. Gething and J. Sambrook, "Protein folding in the cell," *Nature,* vol. 355, pp. 33-45, 1992.

[46] L. Kalé, R. Skeel, M. Bhandarkar, R. Brunner, A. Gursoy, N. Krawetz*, et al.*, "NAMD2: greater scalability for parallel molecular dynamics," *Journal of Computational Physics,* vol. 151, pp. 283-312, 1999.

[47] W. Humphrey, A. Dalke, and K. Schulten, "VMD: visual molecular dynamics," *Journal of Molecular Graphics,* vol. 14, pp. 33-38, 1996.

[48] M. L. Nierodzik and S. Karpatkin, "Thrombin induces tumor growth, metastasis, and angiogenesis: Evidence for a thrombin-regulated dormant tumor phenotype," *Cancer Cell,* vol. 10, pp. 355-362, 2006.

[49] J. R. Comer, D. B. Wells, and A. Aksimentiev, "Modeling nanopores for sequencing DNA," *DNA Nanotechnology: Methods and Protocols,* pp. 317-358, 2011.

[50] A. D. MacKerell, B. Brooks, C. L. Brooks, L. Nilsson, B. Roux, Y. Won*, et al.*, "CHARMM: the energy function and its parameterization," *Encyclopedia of Computational Chemistry,* 1998.

[51] A. D. MacKerell Jr, D. Bashford, M. Bellott, R. L. Dunbrack Jr, J. D. Evanseck, M. J. Field*, et al.*, "All-atom empirical potential for molecular modeling and dynamics studies of proteins†," *The Journal of Physical Chemistry B,* vol. 102, pp. 3586-3616, 1998.

[52] K. Padmanabhan and A. Tulinsky, "An ambiguous structure of a DNA 15-mer thrombin complex," *Acta Crystallogr D Biol Crystallogr,* vol. 52, pp. 272-82, Mar 1 1996.

[53] A. Aksimentiev, "Deciphering ionic current signatures of DNA transport through a nanopore," *Nanoscale,* vol. 2, pp. 468-483, 2010.

[54] D. P. Goldenberg and T. E. Creighton, "Gel electrophoresis in studies of protein conformation and folding," *Analytical Biochemistry,* vol. 138, pp. 1-18, 1984.

[55] W. Berg, B. Hillvärn, H. Arwin, M. Stenberg, and I. Lundström, "The isoelectric point of thrombin and its behaviour compared to prothrombin at some solid surfaces," *Thrombosis and Haemostasis,* vol. 42, pp. 972-982, 1979.

[56] J. C. Phillips, R. Braun, W. Wang, J. Gumbart, E. Tajkhorshid, E. Villa*, et al.*, "Scalable molecular dynamics with NAMD," *Journal of Computational Chemistry,* vol. 26, pp. 1781-1802, 2005.